Acta Mech 223, 1633–1643 (2012)
DOI 10.1007/s00707-012-0636-x

Fabio Casciati · Lucia Faravelli

Experimental investigation on the aging of the base isolator elastomeric component

Received: 1 July 2011 / Revised: 14 November 2011 / Published online: 22 March 2012

Abstract Base isolation is a well-established technique of vibration mitigation. Among the many devices available on the market, elastomeric base isolators are widely adopted. Their drawback is the aging of the elastomeric component, which makes a strict maintenance plan mandatory. This manuscript summarizes an experimental study where the performance of new base isolators is compared with that of 10-years old devices.

List of symbols

a_u	Acceleration of the upper plate (m/s^2)
d	Diameter of rubber disks (mm)
m	Mass (kg)
n	Number of rubber disks
t_r	Total rubber height (mm)
D	Actual device diameter (mm)
G	Elastic shear modulus (MPa)
K	Horizontal stiffness (N/mm)
T	Period (s)
ζ	Viscous damping

1 Introduction

Base isolation was introduced in civil and infrastructure engineering 20 years ago [1–7]. To achieve the isolation goal, several kinds of devices were introduced, studied, tested, and upgraded: several state-of-the-art reports were produced and published [8–16]. Furthermore, the European Standard EN 15129: Anti-seismic devices [17] has been officially adopted since August 1, 2011, by the European Union and other States members of the European Committee for Standardization (CEN). This standard provides performance-based functional requirements (as well as design rules, material characteristics, manufacturing processes, testing procedures, conformity evaluation, and in-service inspections) of hardware to be used in designing and building structures in seismic areas. After several iterations, the existing seismic hardware was subdivided into four functional groups: (i) rigid connection devices; (ii) displacement-dependent devices; (iii) velocity-dependent devices;

Dedicated to Professor Hans Irschik on the occasion of his 60th birthday.

F. Casciati (✉) · L. Faravelli
University of Pavia, Pavia, Italy
E-mail: fabio@dipmec.unipv.it

L. Faravelli
E-mail: lucia@dipmec.unipv.it

and (iv) isolators. The devices in the last group are conceived to support the gravity load of the structure, together with the vertical forces produced by the earthquake action, and to accommodate the large horizontal displacements produced by the seismic excitation.

These isolators are further subdivided into sliders (with either flat or curved surface) and the most popular elastomeric base isolators [18]. The latter ones are made of a sequence of rubber and steel disks between two steel plates. As said, the function is to support heavy vertical loads but also to offer a low stiffness to the load in the horizontal plane. Thus, the period of the global structural system jumps up in a region of the design spectrum characterized by lower excitation intensities.

The adoption of rubber as structural component gave rise to several problems, depending on the nonlinear features of the material constitutive law. But the main issue was immediately identified in the durability due to the aging process of the rubber [19,20].

The available structural codes covering the topic (EN 1998, EN 1337:2006, EN1529:2009 within Europe and NTC 2008 in Italy, that is, [21–23]) deals with the durability asking for tests after 21 days of accelerated aging at 70°C. Accepted is an increase of the elastic shear modulus G (at 100% of deformation) of 15%.

The authors organized more than one decade ago an experimental campaign [24] on elastomeric devices, and some of them were left unused. It was easy, 10 years later, to order from the same producer a new stock of that specific device and to carry out tests on the new and old items in view of a performance comparison [25].

It is worth noticing that reference [26] summarizes a study still undergoing which can be regarded as a full-scale test. The first base isolation system realized in Italy saw some extra-devices, simply put in a vice reproducing the vertical load on the mounted devices, and stored nearby the devices in service. Periodically one or two of them are moved to a laboratory and undergo an experimental campaign.

2 The special device

This study reports tests on base isolators available on the market for applications in the seismic prevention of monumental items, which be of modest volume and weight, as fountains (the “renaissance fountain of San Giuliano di Puglia, Italy”, is sketched in Figs. 1, 2) or statues (the bronzes of Riace, exposed in the national museum of Reggio Calabria, Italy, are shown in Figs. 3, 4).

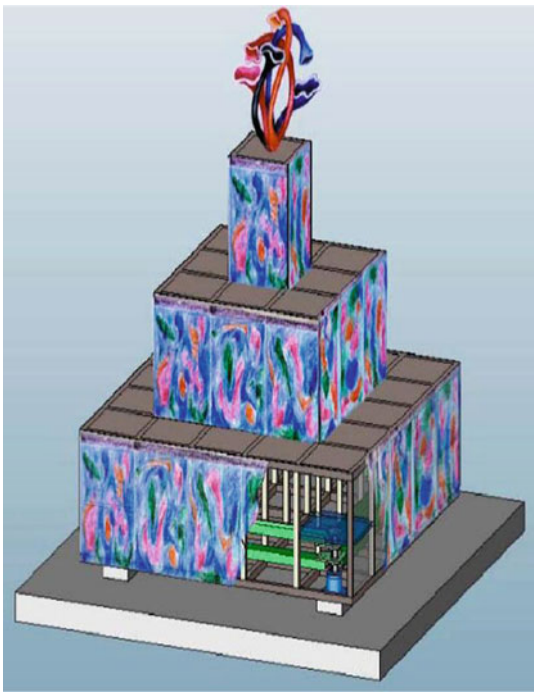

Fig. 1 Renaissance fountain of San Giuliano di Puglia, Italy, with evidence on the a-seismic base isolated supporting frame

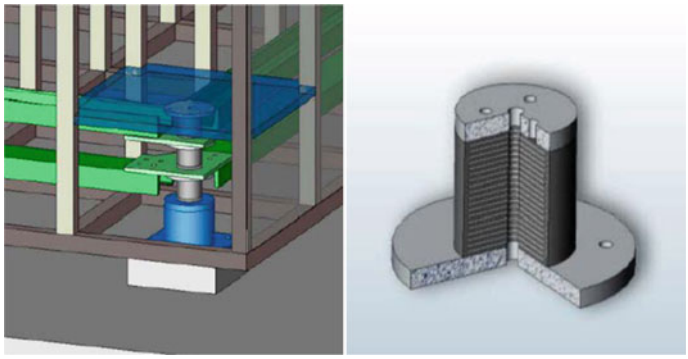

Fig. 2 Detail of Fig. 1 (*left*) and view of the adopted base isolator (*right*)

Fig. 3 The Riace bronzes in the Reggio Calabria (Italy) museum

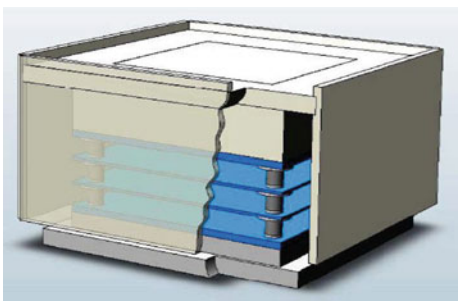

Fig. 4 Detail of the base isolation in Fig. 2

These isolators belong to the class of devices named low damping rubber bearing (LDRB) with a size compatible with the available experimental equipment, which makes possible to avoid any scale-related problems.

They come with the following values of the main parameters:

- number of rubber disks $n = 20$;
- thickness of rubber disks $t = 1.5\,\text{mm}$;
- total rubber height $t_r = 30\,\text{mm}$;
- diameter of rubber disks $d = 55\,\text{mm}$;
- actual device diameter $D = 60\,\text{mm}$;
- elastic shear modulus at 100% of deformation $G = 0.8\,\text{MPa}$;
  - viscous damping $\zeta = 0.1$;
  - resulting stiffness $K = \text{GA}/t_r$.

To provide further details on the elastomeric material under investigation is out from the scope of this study; nevertheless, a further bit of information is provided in the "Appendix".

3 The experimental mock-up

The available mono-axial shaking table, driven by a 407 MTS controller [27], is shown in Fig. 5. The controller relies on an internal linear variable differential transducer (LVDT) measuring the table displacement.

The acquisition of the other kinematic data is obtained by two FA11 Kinemetrics accelerometers. They are mounted directly on the table and on the upper plate, respectively.

The upper plate has a mass of 100 kg and is supported by a single elastomeric device on the left side. On the right side, two steel–Teflon supports guarantee the sliding. This leads to a system period $T = 0.23\,\text{s}$. It is largely lower than the values adopted in actual base isolation design. Larger values of this period, therefore, would have been welcomed, but this can only be obtained by increasing the mass (the shaking table can carry up to 400 kg). Such a mass increase would induce larger frictions on the sliding supports, and the test results would be affected by such an anomalous situation.

The excitation was of the sinusoidal type: the nominal span of the table was always $\pm 10\,\text{mm}$, while the nominal frequency was set at 2, 8, and 10 Hz. For sake of data management, the accelerometers measures were recorded for 500 cycles and stored. The number of collected records are as follows: 50 sets for 2 Hz, 125 sets for 8 Hz, and 5 sets for 10 Hz. Each isolator was submitted to the same sequence, moving from the lower frequency to the upper one.

The expected response sees first the table and the supported plate moving rigidly at 2 Hz, then at 8 Hz, and the upper plate is nearly at rest when the shaking table oscillates, and this is even more evident at 10 Hz.

Before entering the details of the experiment campaign, the next section outlines the reasons that make the elastomeric component aging a central issue when working with rubber base isolators.

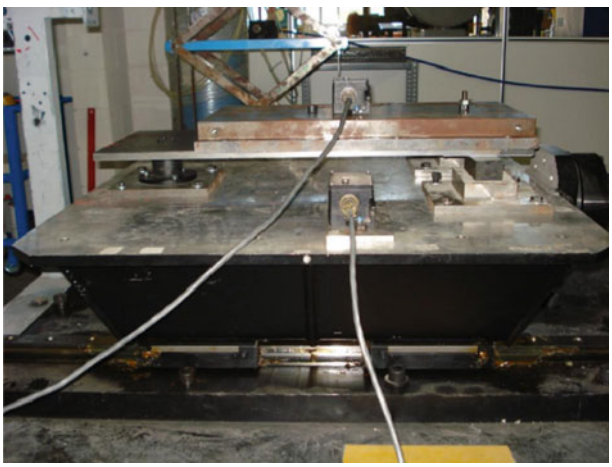

Fig. 5 The experimental mock-up

4 The durability issue

The current structural codes [13,16], valid in all the European Union countries, require from the designer the redaction of a quality plan, covering the different stages of design, construction, installation, check, and maintenance of the devices. This foresees periodic controls and replacement actions during the expected lifetime of the structural system.

Focusing on the durability issue, the aging properties of the elastomeric components, the degradation action of atmospheric oxygen on the surfaces of steel elements, and the physical characteristics of the adhesive employed to fix steel plates and rubber disks are the main concern.

It is worth noticing that the steel elements' surfaces are surrounded by rubber (and hence protected), while the terminal free plates come with a coating protection film (painting), so that their aging is negligible in this specific case study.

By contrast, deteriorations in the adhesive performance and degradations of the elastomeric properties are the significant durability issues, and the only counteraction is the replacement of the entire device.

The degradation of the elastomeric component depends on a long list of parameters. The main ones can be summarized as follows:

(a) initial compound with special reference to the chemical additives; they are mainly added to preserve some properties at very low and/or very high environment temperatures, but affect significantly the aging process;
(b) the mean value and the standard deviation of the compression action induced by the superstructure; it can also be quite different from the design value or vary significantly in time;
(c) the thermal cycles induced by night–day and winter–summer temperature excursions;
(d) local shocks of a thermal or mechanical nature; in particular, fires nearby the device could deteriorate its properties without any visual evidence.

All these aspects influence the increase in time of the shear modulus at 100% deformation, as well as its dependency on the deformation itself, thus affecting also the initial and final transients of vibration.

The base isolator is added in order to introduce bodies of large flexibility: when the time deterioration increases its stiffness, the device replacement becomes a must.

5 Test results

As announced in Sect. 2, two different devices were tested: device 1 was produced in September 2000; device 2 was produced in July 2010. Both devices come from the same company and have the same specifications.

5.1 2 Hz tests

When adopting the lower frequency, the periodogram of Fig. 6 (referred to device 1) shows that the actual excitation frequency is 1.935 Hz. Since the maximum recorded table acceleration is $1.47\,\mathrm{m/s^2}$, the actual span of the piston is obtained after dividing the maximum acceleration by the square of 2π times the frequency, which results in 9.9 mm.

Device 1, the old one, sees the relative displacement in the range +0.5 mm and the inertia force on the plate up to 160 N.

Device 2, the new one, sees the relative displacement in the range +4.0 mm and the inertia force on the plate up to 190 N.

This test is affected by the friction in the sliding supports, friction which dominates the transit across the initial condition during the motion. But in the old device, the effect is no relative motion and no hysteresis cycle, whereas the new device establishes two different hysteresis loops for negative and positive values of the inertia force.

5.2 8 Hz tests

When adopting the nominal frequency of 8 Hz for the excitation, the periodogram of Fig. 7 (referred to device 1) shows that the actual excitation frequency is 7.729 Hz and that the signal intensity is de-amplified moving

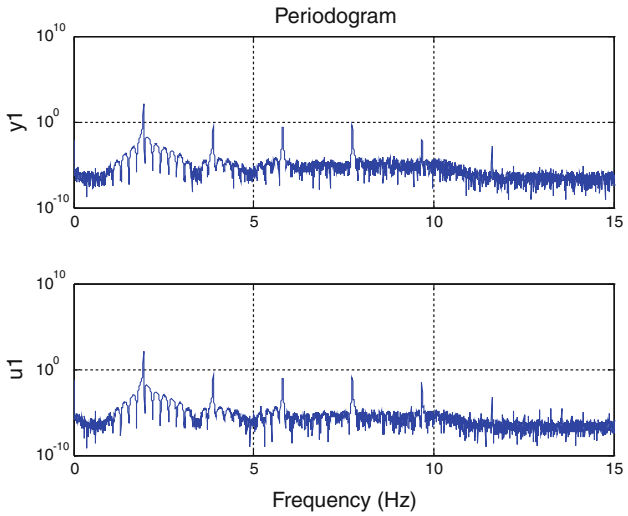

Fig. 6 Periodograms of the acceleration of the table (*bottom*) and of the upper plate (*top*), in the 2 Hz case

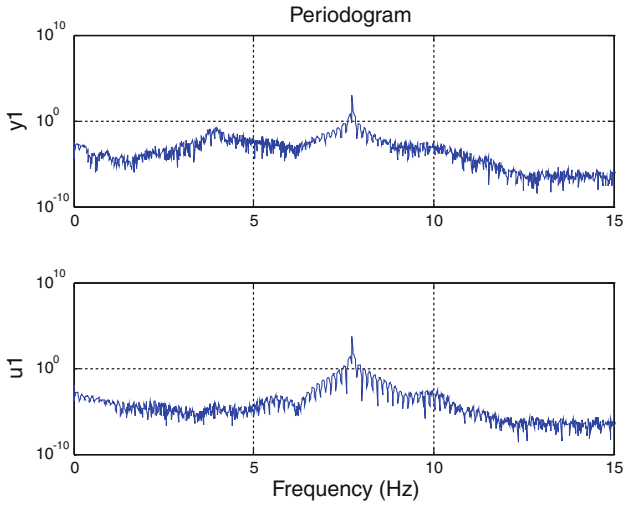

Fig. 7 Periodograms of the acceleration of the table (*bottom*) and of the upper plate (*top*), in the 8 Hz (nominal) case

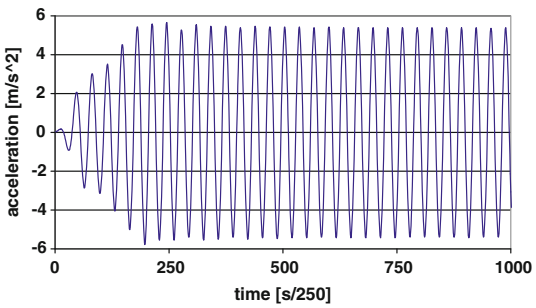

Fig. 8 Acceleration time history recorded by the upper accelerometer when device 1 (2000) is mounted. Excitation nominal frequency: 8 Hz; 250th set of 500 cycles

from the table to the plate, as Fig. 8 (reporting the 250th set of 500 cycles) clarifies. Indeed, the maximum recorded table acceleration is 17.7 m/s^2. The actual span of the piston is obtained after dividing this acceleration value by the square of 2π times the frequency, which results into 7.5 mm (instead of the nominal 10 mm, showing the limit of a shaking table piston designed to work correctly up to 5 Hz, but approximately between 5 and 15 Hz).

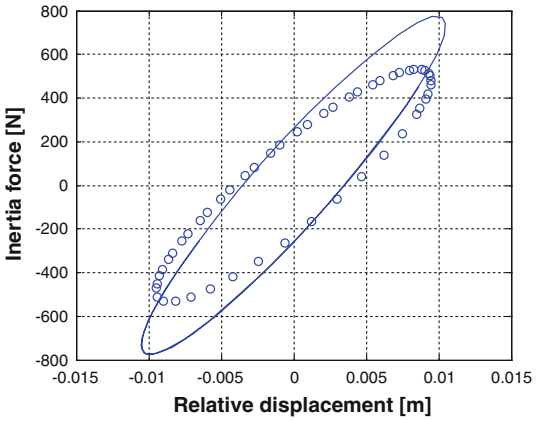

Fig. 9 Hysteresis loop with the relative displacement in the abscissa and the inertia force of the upper plate in the ordinate when device 1 (2000) is mounted. Excitation nominal frequency: 8 Hz. *Solid line*: 50 recording points at the end of the 2nd set of 500 cycles; *circles* at the end of the 200th set

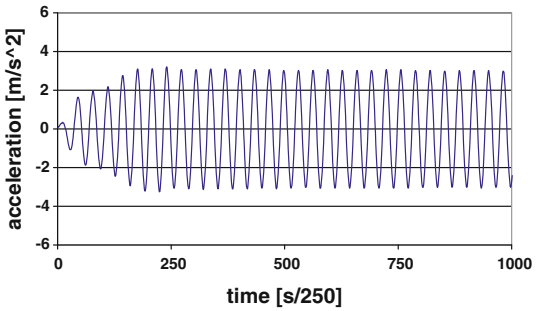

Fig. 10 Acceleration time history recorded by the upper accelerometer when device 2 (2010) is mounted. Excitation nominal frequency: 8 Hz; 250th set of 500 cycles

Device 1, the old one, in the 2nd set of 500 cycles, sees the absolute displacement in the range ± 3 mm but the relative displacement in the range ± 11 mm and the inertia force on the plate up to 800 N. The clockwise hysteresis loop with the relative displacement in the abscissa and the inertia force of the top plate is given in Fig. 9. The solid line refers to 50 recording points at the end of the 2nd set; the circles give the loop at the end of the 200th set. The reduction of the equivalent stiffness is evident.

Device 2, the new one, in the 2nd set of 500 cycles, sees an actual frequency of 7.76 Hz and an actual span of 7.6 mm. Then, the absolute displacement is in the range ± 1.9 mm with the relative displacement in the range ± 9 mm and the inertia force on the plate up to 400 N: it is one half of that of device 1, and this is made evident when comparing Figs. 8 and 10. The hysteresis loop with the relative displacement in the abscissa and the inertia force of the top plate is given in Fig. 9. The solid line refers to 50 recording points at the end of the 2nd set; the circles give the loop at the end of the 200th set. The reduction of equivalent stiffness can still be detected, but its extent is lower than for device 1.

The couple of Figs. 8 and 10 provides the time histories of the acceleration a_u recorded by the upper accelerometer for the two devices, 2000 and 2010, respectively. The values a_u should be compared with the table acceleration that spans in the range $\pm 17.7\,\mathrm{m/s^2}$, that is, the excitation, which is the same in the two cases. Once again one achieves the conclusion that the old device is unable to offer the same quality of the new one in terms of base isolation, since the recorded acceleration is nearly double. This negative feature is confirmed by the couple of Figs. 9 and 11, which outlines a faster deterioration as the loading–unloading cycles proceed for the old device.

5.3 10 Hz details

Finally, adopting the nominal frequency of 10 Hz for the excitation, the periodogram of Fig. 12 (referred to device 1) shows that the actual excitation frequency is 9.658 Hz and that the signal intensity is de-amplified moving from the table to the plate, as Fig. 13 (reporting the 5th set of 500 cycles) clarifies. Indeed, the

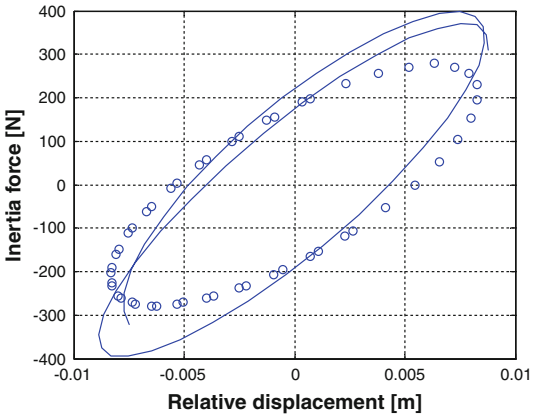

Fig. 11 Hysteresis loop with the relative displacement in the abscissa and the inertia force of the upper plate in the ordinate when device 2 (2010) is mounted. Excitation nominal frequency: 8 Hz. *Solid line*: 50 recording points at the end of the 2nd set of 500 cycles; *circles* at the end of the 200th set

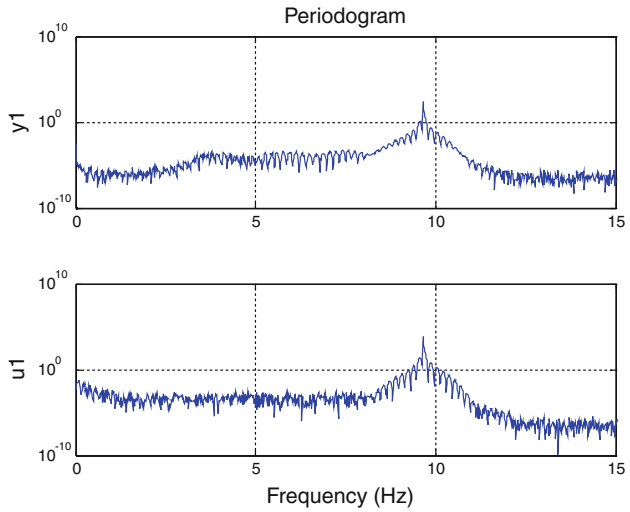

Fig. 12 Periodograms of the acceleration of the table (*bottom*) and of the upper plate (*top*), in the 10 Hz (nominal) case

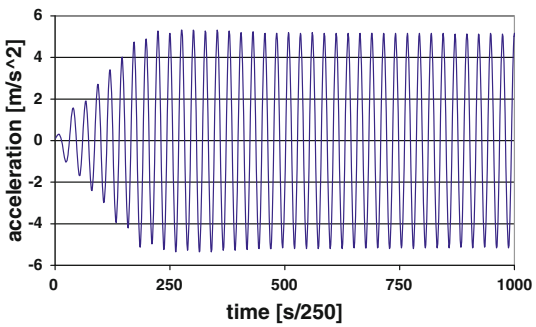

Fig. 13 Acceleration time history recorded by the upper accelerometer when device 1 (2000) is mounted. Excitation frequency: 10 Hz; 2nd set of 500 cycles

maximum recorded table acceleration is 25.35 m/s^2. The actual span of the piston is obtained after dividing this acceleration value by the square of 2π times the frequency, resulting in 6.9 mm (instead of the nominal 10 mm).

Device 1, the old one, in the 2nd set (over 5) of 500 cycles, sees the absolute displacement in the range ± 1.5 mm with the relative displacement in the range ± 8.2 mm and the inertia force on the plate up to 500 N. The clockwise hysteresis loop with the relative displacement in the abscissa and the inertia force of the top

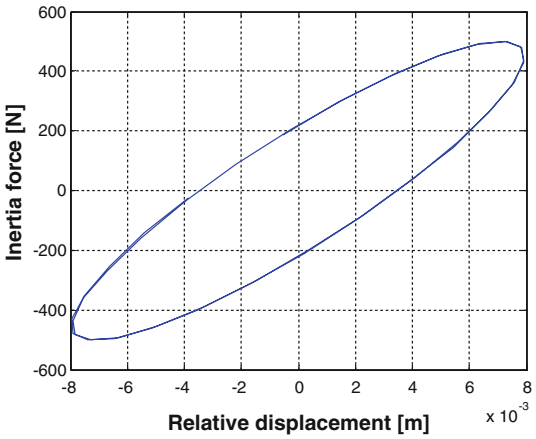

Fig. 14 Hysteresis loop with the relative displacement in the abscissa and the inertia force of the upper plate in the ordinate when device 1 (2000) is mounted. Excitation frequency: 10 Hz. *Solid line*: 50 recording points at the end of the 2nd set of 500 cycles

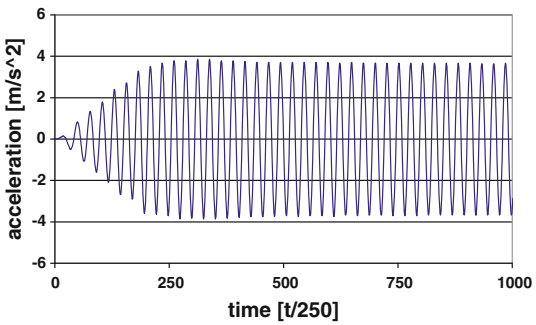

Fig. 15 Acceleration time history recorded by the upper accelerometer when device 2 (2010) is mounted. Excitation frequency: 10 Hz; 2nd set (over 5) of 500 cycles

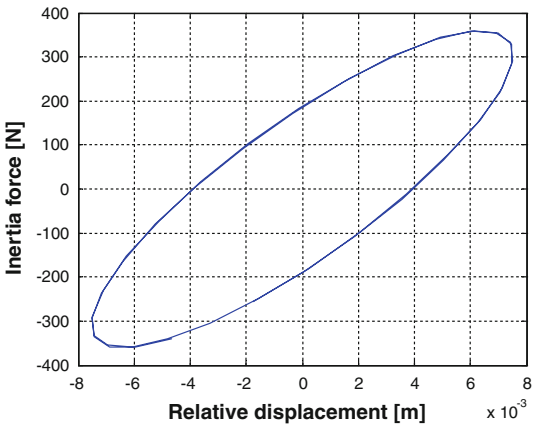

Fig. 16 Hysteresis loop with the relative displacement in the abscissa and the inertia force of the upper plate in the ordinate when device 2 (2010) is mounted. Excitation frequency: 10 Hz. *Solid line*: 50 recording points at the end of the 2nd set of 500 cycles

plate is given in Fig. 14. The solid line refers to 50 recording points at the end of the 2nd set; the circles give the loop at the end of the 2nd set. The reduction of the equivalent stiffness is evident.

Device 2, the new one, in the 2nd set of 500 cycles, sees an actual frequency of 9.652 Hz and an actual span of 6.9 mm. Then, the absolute displacement in the range ± 1 mm with the relative displacement in the range ± 7.75 mm and the inertia force on the plate up to 360 N (see Fig. 15). The hysteresis loop with the relative displacement in the abscissa and the inertia force of the top plate is given in Fig. 16. The solid line refers to 50 recording points at the end of the 2nd set. Even in this case, a reduction of the equivalent stiffness can be detected.

The acceleration of the isolated system is even lower in the case of the old device (device 1), thus showing that the 100% deformation material response is reached, in this case, for a peak acceleration larger than that of device 2. The latter device, by contrast, sees just a light increase of the response acceleration range when comparing the time histories in Figs. 13 and 15.

6 Conclusions

This study provides the first results of an experimental campaign where the response of base isolators, built by the same company today and 10 years ago, is compared.

The expected increase of the device stiffness was recorded and is underlined in this study. A large amount of collected data, however, were collected. Their future processing could make possible:

(1) to balance maintenance (replacement) plans with the targeted system reliability and
(2) to check the accuracy of the tests required by existing codes in view of incorporating the aging aspects and to ensure durability of the isolators.

Acknowledgments This research is supported by a grant from the Italian Ministry of Public Instruction and by grants which made possible the stay of foreign students at the authors' institution. The authors are also indebted with ALGA spa, Milan, Italy, for providing them the new lot of devices without any charge.

Appendix: Details on the used elastomeric material

The reader is addressed to page 115 of the book by Kelly [18] for a plot of the shear stress as function of the shear strain of the elastomeric component. One sees a plot increasing from 0 to 0.35 MPa when the strain goes from 0 to 50%. A second branch (flatter than the first one) spans up to 250% of strain reaching 1.41 MPa of stress. The third branch goes up to 560% of strain and 7 MPa of stress. The ratio between increment of stress and increment of strain provides an estimate of the shear modulus (G) value at 100% of deformation.

Table 1 Physico-mechanical properties of the compounds used for base isolations

Characteristics		Compound		
		Soft	Normal	Hard
Hardness	Shore A3	40 ± 3	40 ± 3	40 ± 3
Tensile strength	MPa	20	20	18
Ultimate strain	%	750	600	500
G modulus	MPa	0.4	0.8	1.4
Equivalent viscous damping	%	10	10	16

Table 1 provides the market alternatives adopted in the assemblage of base isolators: the central column defines all the features of the elastomeric component which was used to build the tested devices.

References

1. Buckle, I.G., Mayes, R.L.: Seismic isolation history: application and performance—a world review. Earthq. Spectra **6**, 161–201 (1990)
2. Bettinali, F., Bonacina, G., Pucci, G., Serino, G., Giuliani, G.C., Forni, M., Indirli, M., Martelli, A.: On-site dynamic test of a large seismically isolated building and related numerical analysis. In: Proceedings of ASME Pressure Vessel and Piping Conference, San Diego, CA, USA, 23–28 June 1991, PVP-vol. 222, pp. 77–89 (1991)
3. Skinner, R.I., Robinson, W.H., McVerry, G.H.: An Introduction to Seismic Isolation. Wiley, New York, NY (1993)
4. Casciati, F., Lagorio, H.J.: Urban renewal aspects and technological devices in infrastructure rehabilitation. In: Proceedings of the First European Conference on Structural Control, Barcellona; World Scientific, Singapore, pp. 173–181 (1996)
5. Soong, T.T., Dargush, G.F.: Passive Energy Dissipation in Structural Engineering. Wiley, New York, NY (1997)
6. Casciati, F., Magonette, G., Marazzi, F.: Technology of Semiactive Devices and Applications in Vibration Mitigation. Wiley, Chichester (2006)
7. Casciati, F., Faravelli, L.: A passive control device with SMA components: from the prototype to the model. J. Struct. Control Health Monit. **16**(7–8), 751–765 (2009)

8. http://nisee.berkeley.edu/lessons/kelly.html
9. Kelly, J.M.: Seismic isolation systems for developing countries. Earthq. Spectra **18**(3), 385–406 (2002)
10. Yoshida, J., Abe, M., Fujino, Y., Watanabe, H.: Three-dimensional finite-element analysis of high damping rubber bearing. J. Eng. Mech. ASCE **130**(5), 607–620 (2004)
11. Nagarajaiah, S., Sahasrabudhe, S.: Seismic response control of smart sliding isolated buildings using variable stiffness systems: an experimental and numerical study. Earthq. Eng. Struct. Dyn. **35**(2), 177–197 (2006)
12. Narasimhan, S., Nagarajaiah, S., Johnson, E.A., Gavin, H.P.: Smart base-isolated benchmark building. Part I: problem definition. J. Struct. Control Health Monit. **13**(2–3), 573–588 (2006)
13. Sannino, U., Sandi, H., Martelli, A., Vlad, I.: Modern systems for mitigation of seismic action. In: Proceedings of the Symposium Held at Bucharest, Rumania, 31 Oct 2008, ISBN 978-973-720-223-9, AGIR Publishing House, Bucharest (2009)
14. Fadi, F., Constantinou, M.C.: Evaluation of simplified methods of analysis for structures with triple friction pendulum isolators. Earthq. Eng. Struct. Dyn. **39**(1), 5–22 (2009)
15. Morgan, T.A., Mahin, S.A.: Achieving reliable seismic performance enhancement using multi-stage friction pendulum isolators. Earthq. Eng. Struct. Dyn. **39**(13), 1443–1461 (2010)
16. Chang, C.-M., Spencer, B.F.: Active base isolation of buildings subjected to seismic excitations. Earthq. Eng. Struct. Dyn. **39**(13), 1493–1512 (2010)
17. CEN (European Committee for Standardization): EN 15129:2009—Anti-seismic Devices, Austrian Standards Institute, Wien (2010)
18. Kelly, J.M.: Earthquake-Resistant Design with Rubber. Springer, London (1993)
19. Barker, L.R.: Accelerated long-term ageing of natural rubber vulcanizates. Part 2: results from ageing tests at 40°C. Rubber Dev. **44**(2/3), 91 (1991)
20. Fuller, K.N.G., Pond, T.J.: The Long Term Performance of High Damping Natural Rubber Seismic Bearings, European Seismic Design Practice. Balkema, Rotterdam (1995)
21. CEN: EN 1998 (Eurocode 8), Design of structures for earthquake resistance
22. CEN: EN 1337:2006, Structural bearings—general design rules
23. Italian Infrastructures Ministry Decree: Norme Tecniche per le Costruzioni 2008 (in Italian), Gazzetta Ufficiale 29, 04-02-2008 (2008)
24. D'Andrea, A.: Identificazione del comportamento di dispositivi elastomerici per l'isolamento alla base (in Italian). Civil engineering master thesis, University of Pavia (1998)
25. Andena, J.: Invecchiamento del componente elastomerico in dispositivi di isolamento alla base (in Italian). Civil engineering master thesis, University of Pavia (2010)
26. Bergamo, G., Forni, M.: Effetti dell'invecchiamento naturale sugli isolatori sismici elastomerici ad elevato smorzamento del Centro Regionale Telecom di Ancona (in Italian). http://www.assisi-antiseismicsystems.org/.../GN11/GN11_Invecchiamento.pdf
27. MTS 407: User manual (1994)